DOI: 10.1002/adsc.200700367

Density Functional Theory Study of the *Cinchona* Thiourea-Catalyzed Henry Reaction: Mechanism and Enantioselectivity

Peter Hammar,[a] Tommaso Marcelli,[b] Henk Hiemstra,[b] and Fahmi Himo[a,*]

[a] Department of Theoretical Chemistry, School of Biotechnology, Royal Institute of Technology, SE-106 91 Stockholm, Sweden
Fax: (+46)-8-5537-8590; e-mail: himo@theochem.kth.se
[b] Van't Hoff Institute of Molecular Sciences, University of Amsterdam, Nieuwe Achtergracht 129, 1018 WS Amsterdam, The Netherlands

Received: July 26, 2007; Published online: November 27, 2007

Dedicated to Professor Jan Bäckvall on the occasion of his 60th birthday.

Supporting information for this article is available on the WWW under http://asc.wiley-vch.de/home/.

Abstract: We report a density functional theory investigation of the enantioselective *Cinchona* thiourea-catalyzed Henry reaction of aromatic aldehydes with nitromethane. We show that two pathways (differing in the binding modes of the reactants to the catalyst) are possible for the formation of the C–C bond, and that they have comparable reaction barriers. The enantioselectivity is investigated, and our results are in agreement with the experimentally observed solvent dependence of the reaction.

Keywords: *Cinchona* alkaloids; density functional theory; enantioselectivity; nitroaldol reaction; organocatalysis

Introduction

The reaction between an enolizable nitroalkane and a carbonyl compound, known as the Henry or nitroaldol reaction, is a very important synthetic tool for the creation of a carbon-carbon bond and up to two contiguous stereogenic centers.[1] Traditionally, like the aldol reaction, this reaction was mainly carried out in the presence of strong bases, leading to dehydration with concomitant formation of a nitroolefin. The interest in asymmetric versions of this reaction started growing after the groundbreaking work of Shibasaki and co-workers on the use of chiral bimetallic lithium-lanthanum catalysts.[2] In the last two decades many other asymmetric metal catalysts have been developed: nowadays, aldehydes or α-keto esters can be converted to the corresponding nitroalcohols with mostly excellent enantio- and diastereoselectivity.[3]

On the other hand, the number of efficient asymmetric organocatalysts for the Henry reaction is considerably lower.[4] Our interest in this reaction started with the observation that *Cinchona* alkaloids bearing a phenol on the C-6′ position (cupreines)[5] are moderately enantioselective bifunctional organocatalysts for the addition of nitromethane to activated aromatic aldehydes.[6] Replacement of the phenol with a better hydrogen bonding moiety such as an electron-poor thiourea[7] led to a dramatic improvement in both scope and enantioselectivity: organocatalyst **1** was shown to promote the addition of nitromethane to aromatic and heteroaromatic aldehydes in consistently high yields and enantiomeric excesses (Scheme 1).[8]

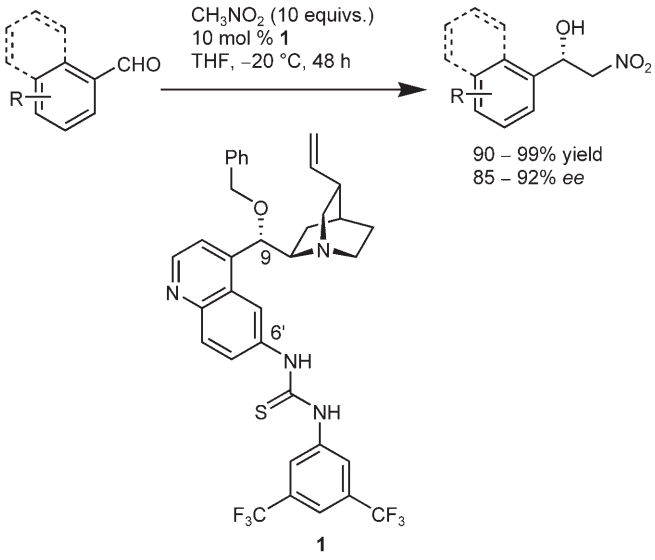

Scheme 1. *Cinchona* thiourea-catalyzed enantioselective Henry reaction.

In the same period, Nagasawa and co-workers developed a guanidine-thiourea catalyst giving excellent results in the Henry reaction of aliphatic aldehydes[9] and Deng and co-workers showed that simple cupreines are highly enantioselective catalysts for the addition of nitromethane to α-keto esters.[10] More recently, Griengl and co-workers obtained high stereoselectivities using the hydroxynitrile lyase extracted from *Hevea brasiliensis* as biocatalyst for the Henry reaction of selected aldehydes with nitromethane and nitroethane.[11]

Despite the impressive advancement of asymmetric organocatalysis in these last years,[12] the mechanisms of most organocatalytic transformations have not been investigated in detail. While considerable efforts have been applied to the understanding of amino acid-catalyzed reactions, mechanistic studies on *Cinchona*-derived organocatalysts are scarce.[13]

In this paper we report a theoretical study of the *Cinchona* thiourea-catalyzed Henry reaction, aimed at the elucidation of the mode of action of this catalyst and the origins of the enantioselection. We employ the density functional theory (DFT) of B3LYP,[14] which has become the method of choice for this kind of studies, as it yields accurate geometries and energies. Accordingly, it has been used in a number of investigations of organocatalytic reactions.[15]

The reaction we considered in the present study is the addition of nitromethane to benzaldehyde (**2**), yielding nitroalcohol **3** (Scheme 2).

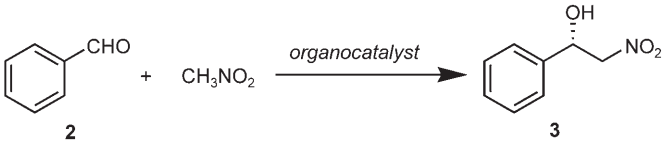

Scheme 2. Henry reaction of benzaldehyde with nitromethane considered in the present paper.

Computational Details

All calculations were performed using the hybrid density functional theory method B3LYP as implemented in the Gaussian03 program package.[16] Geometries were optimized with the 6-31G(d,p) basis set, and characterized by frequency calculations. Final energies were calculated using a larger basis set, 6-311+G(2d,2p), and corrected for zero-point vibrational effects obtained from the frequency calculations.

The effect of solvation was calculated as single point energies using the CPCM polarizable continuum model[17] with THF ($\varepsilon = 7.58$) as solvent, and was added as a correction to the final energies.

Results and Discussion

Model Catalyst

In order to reduce the computational costs for the calculations described below, we decided to employ a slightly simplified catalyst. We envisaged that the benzyloxy substituent on C-9 could be replaced by a methoxy group and that removal of the trifluoromethyl groups on the thiourea part would have provided a catalyst leading to still considerable asymmetric induction. To corroborate this, we synthesized thiourea **4** (Figure 1). Its use in the Henry reaction of benzaldehyde with nitromethane provided nitroalcohol **3** in 73% *ee*. Although this enantiomeric excess is slightly lower compared to that obtained with thiourea **1** (89%), this result is sufficient to justify removal of both a phenyl ring and two trifluoromethyl groups to model the asymmetric Henry reaction.

Thiourea **1** and its pseudoenantiomeric quinine-derived counterpart show nearly perfect enantiomeric behaviour.[8] Therefore, we also removed from our model the vinyl fragment of the quinuclidine, assuming no specific role in the enantioselection process.

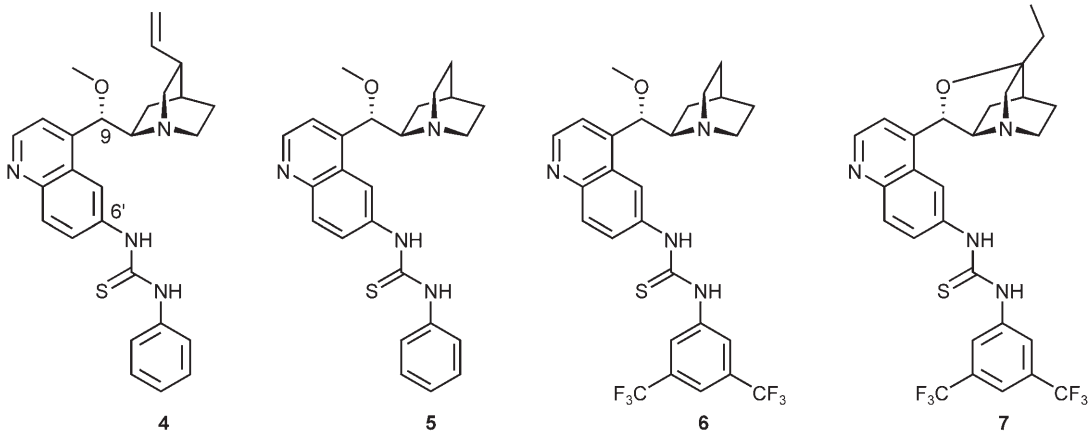

Figure 1. Structures of the catalysts considered in this study.

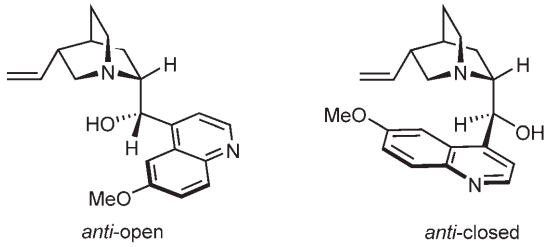

Figure 2. The open and closed conformations of quinidine.

Compound **5** (59 atoms) was therefore chosen as the main computational model for thiourea **1** in the study of the reaction mechanism and stereoselectivity. At a later stage, we introduced back the trifluoromethyl substituents and recalculated a number of the C–C bond forming transition states, to investigate their role on the enantioselection. Compound **6** (65 atoms) was accordingly used in those calculations.

Cinchona alkaloids exist in solution as a mixture of rapidly interconverting conformers.[18] One issue that has to be considered when modeling reactions catalyzed by this class of compounds is the determination of which conformation is adopted by the catalyst (Figure 2).

Due to its tricyclic structure, catalyst **7**[19] cannot adopt closed conformations. Reaction of benzaldehyde catalyzed by 10 mol% thiourea **7** proceeded with moderate yet considerable asymmetric induction (65% *ee*). We judged this result in agreement with the catalyst being in an open conformation. Similar arguments were used by Deng et al. to justify the proposal of an open arrangement in the transition state of the cupreidine-catalyzed addition of substituted β-dicarbonyl compounds to nitroalkenes.[20]

In the density functional calculations described below we did not consider the open conformation with the quinuclidine nitrogen pointing in the opposite direction with respect to the thiourea moiety (*syn*-open) as it would not have been productive during the C–C bond forming step assuming simultaneous coordination of both reactants.

Mechanism

The generally accepted mechanism for the Henry reaction involves deprotonation of nitromethane, and the subsequent C–C bond formation, which is followed by protonation of the product and the regeneration of the catalyst.

Step 1: Deprotonation

The first step of the reaction is the deprotonation of nitromethane by the quinuclidine nitrogen, the most basic site in the catalyst. The enthalpic gain for bringing together nitromethane and the catalyst (complex **I**, Figure 3) is calculated to be 6.8 kcal mol^{-1} in the gas phase, which is reduced to only 1.1 kcal mol^{-1} when solvation is considered, in the form of a dielectric continuum with a dielectric constant of $\varepsilon = 7.58$, corresponding to THF. We note that the nitro group coordinates to the thiourea moiety of the catalyst in a bidentate fashion and the α-protons are suitably positioned in proximity of the quinuclidine nitrogen. From there, the barrier for the proton transfer is calculated to be 14.7 kcal mol^{-1} in gas phase and 10.8 kcal mol^{-1} in solvent. The optimized transition state (**II**) structure is shown in Figure 3. At the TS, an ion pair (nitromethide and protonated catalyst) is created. The critical C–H bond distance is 1.64 Å and the N–H bond distance is 1.16 Å. Due to the high

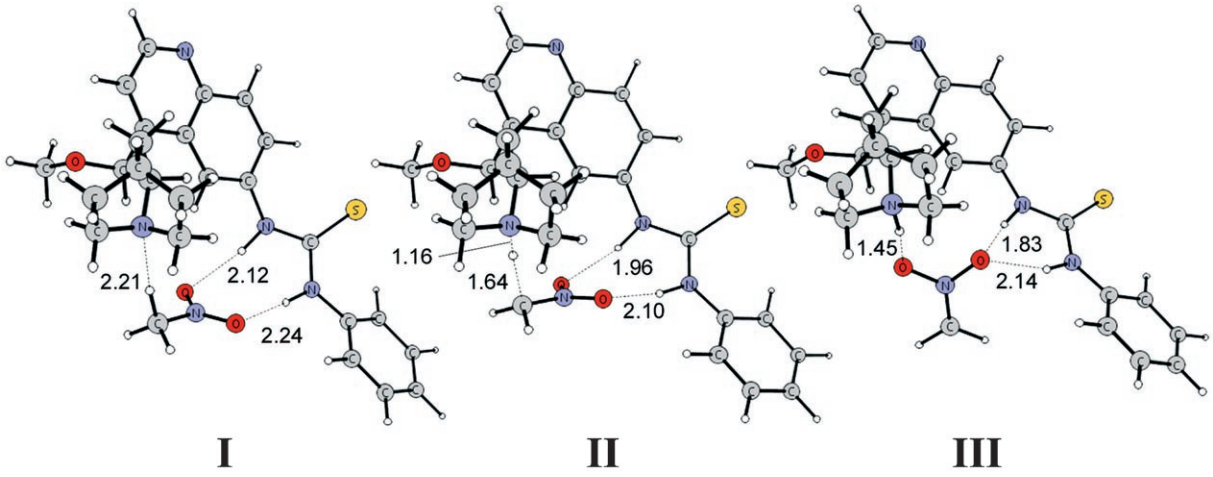

Figure 3. Optimized structures of the stationary points for the proton transfer from the nitromethane to the quinuclidine of the catalyst. Nitromethane bidentately coordinated to the thiourea of the catalyst (**I**); the transition state for the proton transfer (**II**); nitromethide coordinated to the quinuclidinium and the thiourea (**III**).

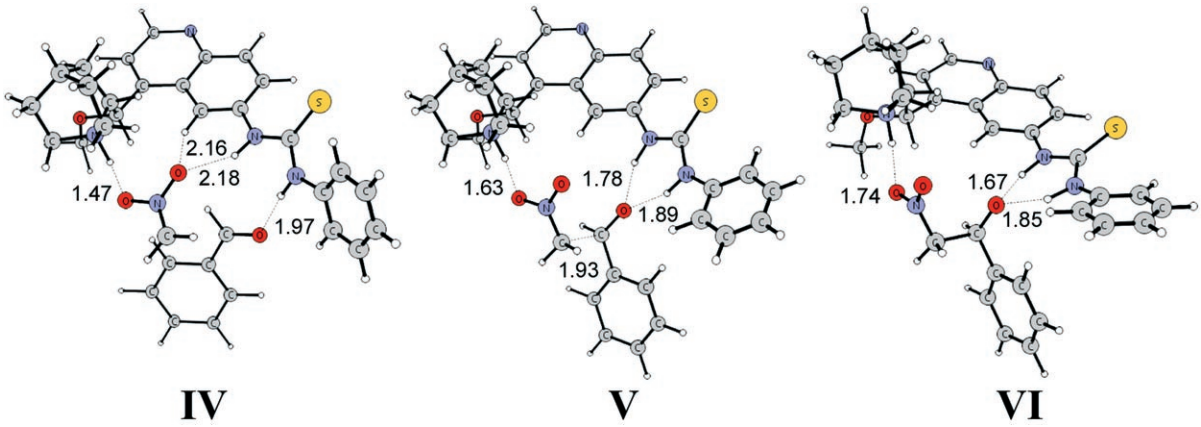

Figure 4. Structures of the stationary points for the C–C bond forming step of Pathway A. Both substrates coordinated to the catalyst (**IV**), the transition state for C–C bond formation (**V**), the intermediate coordinated to the protonated catalyst (**VI**).

degree of charge separation at the TS, it is likely that geometry optimization of the TS in solution will yield somewhat different distances, but this is assumed not to affect the calculated energetics. The negative charge that is developing on the nitromethane causes the hydrogen bonds between the nitro group and thiourea to be shorter, 1.96 and 2.10 Å, compared to 2.12 and 2.24 Å.

The reaction step is found to be slightly exothermic (1.7 kcal mol^{-1}) when solvation is considered, but endothermic by 2.4 kcal mol^{-1} in the gas phase, due to the poor stabilization of the resulting ion pair in the gas phase. These results demonstrate that the first step is energetically feasible.

It is instructive here to consider the relative pK_a values of the species involved in the reaction step. Experimentally, nitromethane has a pK_a value of 17.2, while the pK_a of quinuclidinium is 9.8.[21] The difference is thus 7.4 units, which corresponds to a reaction energy of *ca* +10 kcal mol^{-1}. The complexation of the ion pair (nitromethide and the protonated catalyst) is thus quite strong, leading to a slightly exothermic reaction step.

Step 2: C–C Bond Formation

As demonstrated by Papai and co-workers for conjugate additions, in tertiary amine/thiourea organocatalysis two distinct modes of binding of the electrophile and nucleophile to the catalyst leading to two distinct routes to C–C bond formation can be envisioned.[22]

In the first, called Pathway A, the nucleophilic nitromethide anion is coordinated to the positively-charged trialkylammonium, while the aldehyde electrophile is coordinated to the thiourea moiety (Figure 4). In the second binding mode, called Pathway B, the opposite coordination pattern is found (Figure 5).

Pathway A: When benzaldehyde is bound to the ion pair complex **III** in the fashion shown in Figure 4 (**IV**, Pathway A) a small enthalpic gain is calculated in the gas phase (1.1 kcal mol^{-1}). However, when the solvation effects are included, this becomes an enthalpic penalty of 3.6 kcal mol^{-1}. As seen from Figure 4, the nitro group of the nitromethide forms hydrogen bonds to both the quinuclidinium proton and one of the thiourea hydrogens, while the aldehyde oxygen forms a hydrogen bond to the other nitrogen.

For Pathway A we have calculated all possible transition states (6 in total) for the formation of the C–C bond: these are discussed in detail in the stereochemistry subsection below. The TS with the lowest energy leads to the *S*-product and is depicted in Figure 4 (**V**). Compared to complex **IV**, it has a calculated barrier of 11.2 kcal mol^{-1} in the gas phase, and 8.9 kcal mol^{-1} in solution, which, added to the 3.6 kcal mol^{-1} enthalpic penalty of binding, results in a total barrier of 12.5 kcal mol^{-1} including solvation. Kinetic analysis of the reaction of *p*-trifluoromethylbenzaldehyde with nitromethane catalyzed by **1** showed first-order in both substrates and catalyst (see Supporting Information), in agreement with C–C bond formation being the rate-limiting step.

At the transition state, the critical C–C bond distance is 1.93 Å, and the interaction between the nitromethide and the thiourea is lost in favour of a double hydrogen bond between the thiourea and the aldehyde carbonyl, to better stabilize the developing anion.

The resulting intermediate (**VI**) is only 0.3 kcal mol^{-1} lower than the TS in the gas phase and 1.5 kcal mol^{-1} when solvation is considered. This coordination does not allow any proton transfer but, due to the high basicity of the alkoxide compared to the other species present, protonation is assumed to be a fast event once the product is released from the cata-

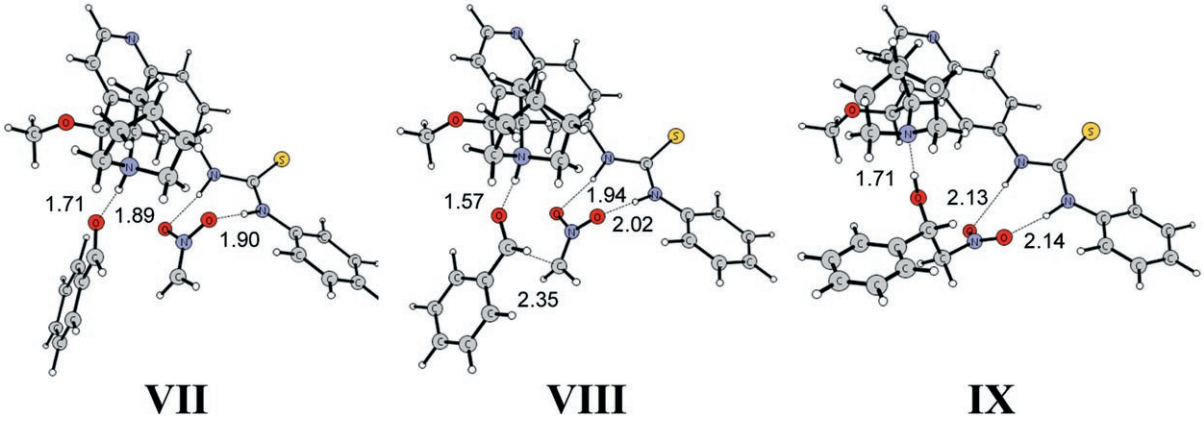

Figure 5. Structures of the stationary points for the C–C bond forming step of Pathway B. Both substrates coordinated to the catalyst (**VII**), the transition state for C–C bond formation (**VIII**), the protonated product coordinated to the regenerated catalyst (**IX**).

lyst. The protonated product (which is the same for Pathways A and B, see Figure 5) is 13.8 kcal mol^{-1} lower than the unprotonated intermediate **VI** in solvent, and 19.5 kcal mol^{-1} in the gas phase.

Pathway B: Considering the corresponding stationary points leading to the *S*-product for Pathway B, it can be noted that the binding of benzaldehyde to the ion pair complex **III** in the fashion shown in Figure 5 (**VII**, Pathway B) results in a larger enthalpic penalty, calculated to 9.6 kcal mol^{-1} in the gas phase and 10.5 kcal mol^{-1} when solvent is considered. Clearly, this binding mode is unfavoured compared to complex **IV**, which has a strong interaction between the positive and negative charges.

On the other hand, the barrier for the C–C bond formation starting from this structure is quite low, calculated to 1.6 kcal mol^{-1} in the gas phase and 3.6 kcal mol^{-1} in solution for the *S*-product (stereochemistry discussed below). The total barrier (11.2 and 14.1 kcal mol^{-1} in the gas phase and solution, respectively) is thus only 1.6 kcal mol^{-1} higher than for Pathway A, indicating that both pathways are quite viable.

At the transition state (**VIII**), the critical C–C bond distance is 2.35 Å, considerably longer than for Pathway A. As a result of the charge development on the aldehyde oxygen atom, the hydrogen bond to the quinuclidinium is shorter, 1.57 Å compared to 1.71 Å in reactant **VII**. The hydrogen bonds of the nitro group to the thiourea moiety, on the other hand, are slightly longer (1.94 and 2.02 Å compared to 1.89 and 1.90 Å).

For this reaction step, no intermediate could be located in gas phase. Instead the proton was found to transfer to the alkoxide at the same transition state, resulting in the protonated product **IX**.

The overall reaction between nitromethane and benzaldehyde yielding nitroalcohol **3**, was calculated to be almost thermoneutral (−0.7 kcal mol^{-1} in the gas phase and +1.2 kcal mol^{-1} when solvent is considered), in good agreement with the well-known reversibility of the Henry reaction. This means that the protonated product **IX** is bound to the catalyst by 6.7 kcal mol^{-1} in solvent (13.5 kcal mol^{-1} in the gas phase).

Scheme 3 summarizes the two mechanistic pathways, and Figure 6 summarizes the energies obtained from the calculations.

Stereoselectivity of C–C Bond Formation

Experimentally, it was previously found that the enantiomeric excess of Henry product **3** is strongly dependent on the reaction medium.[8] This is not an uncommon phenomenon in organocatalysis. However, in most cases such an effect can be readily rationalized in terms of solvent polarity. For the asymmetric Henry reaction, such a correlation was not possible. For instance, THF and dichloromethane are both aprotic solvents having similar dielectric constants yet their use in the Henry reaction at room temperature led to the formation of **5** in 62% and 6% *ee*, respectively. On the other hand, enantiomeric excesses roughly correlate with the Lewis basicity of the solvent, according to the experimental scale compiled by Maria and Gal, using boron trifluoride as the reference Lewis acid (Figure 7).[23] The Lewis basicity for toluene (5% *ee*) is not available but it is reasonable to assume a very low basicity since its donor number (DN, the Lewis basicity determined using $SbCl_5$ as the reference Lewis acid) is small: DN for toluene is 0.1 kcal mol^{-1} compared to 2.7 kcal mol^{-1} for nitromethane and 20.0 kcal mol^{-1} for THF.[24] Methanol is also not included in this scale because it is a protic solvent. As seen from Figure 7, it is clear that solvents of

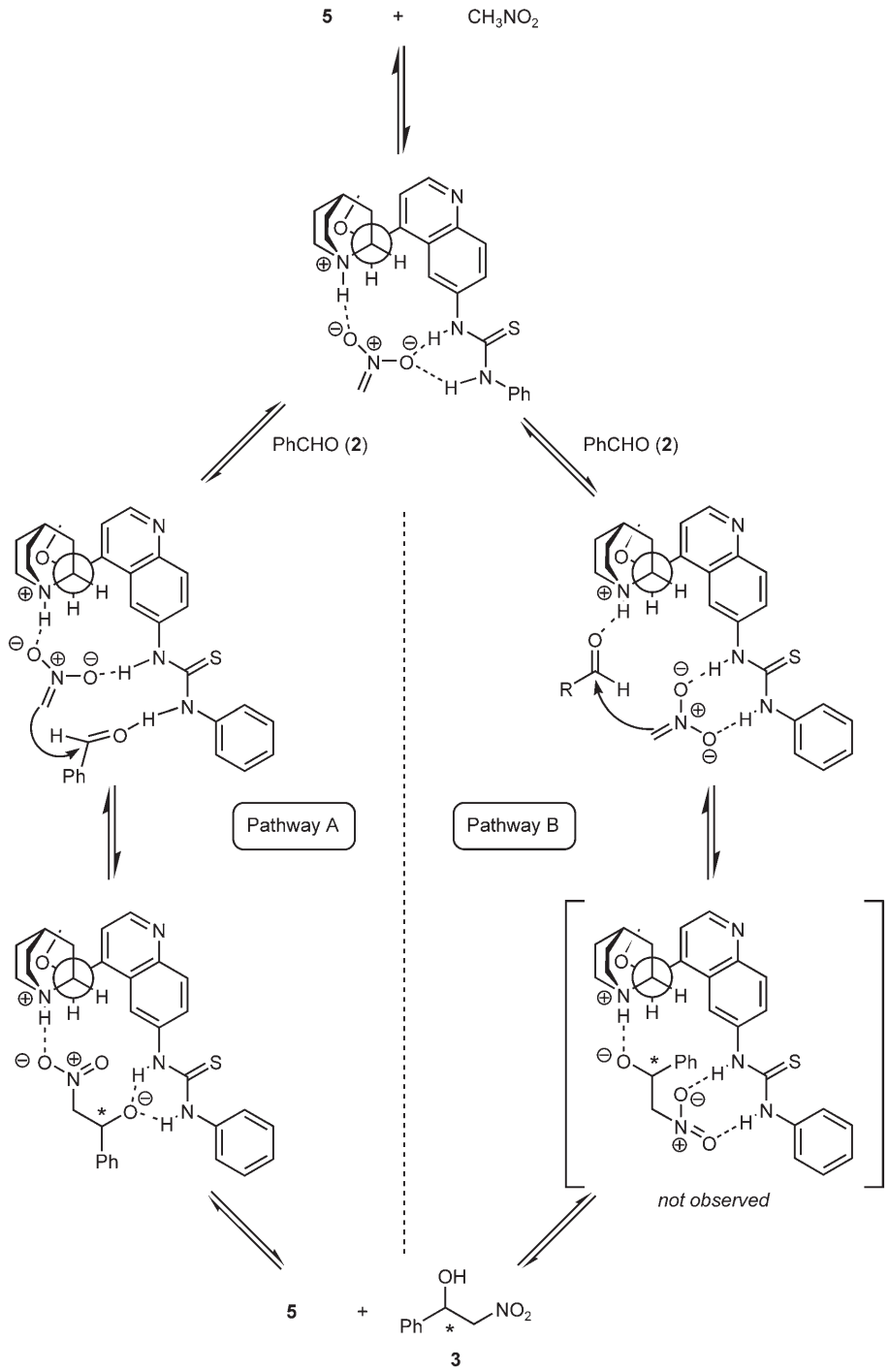

Scheme 3. Proposed mechanisms for the *Cinchona* thiourea-catalyzed Henry reaction.

higher Lewis basicity than nitromethane lead to considerable asymmetric induction. The exact reason for this still remains to be uncovered.

Overall, the high solvent sensitivity of the enantioselectivity indicates the energies of the transition states leading to the *S* and *R* stereomers of the product are very close. Seemingly small differences in the solvent properties can thus induce large changes in the *ee*.

In the present study, we have located the transition states leading to both enantiomers for the two pathways. In the case of Pathway A, we can envision three TS rotamers for each enantiomer (Figure 8, $\mathbf{TS}_{S1}$–$\mathbf{TS}_{R3}$), corresponding to the different Newman projections for C–C bond formation. For Pathway B, the

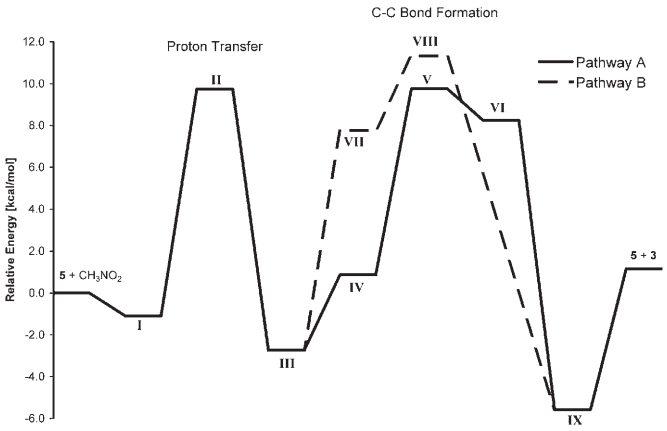

Figure 6. Calculated reaction energy profile (including solvation) for the two pathways.

conformational restriction imposed by the bidentate hydrogen bonds between the thiourea and the nitro group of the nitromethide allows only for one TS for each enantiomer (Figure 8, $\mathbf{TS}_{S4}$ and $\mathbf{TS}_{R4}$), both having the phenyl group of benzaldehyde and the nitro group of nitromethide anion in a *trans*-arrangement.

We first note that the TS with the lowest energy ($\mathbf{TS}_{S1}$) corresponds to the *S*-product, in agreement with the experimental findings. The calculated energy difference to the lowest TS corresponding to the *R*-product is quite small, only 1.1 kcal mol^{-1} ($\mathbf{TS}_{R1}$), also in good agreement with the experiments and with the general conclusions from the solvent studies, namely that the energies of the transition states leading to the different products must be close.

At the preferred transition state ($\mathbf{TS}_{S1}$) the forming C–C bond has a distance of 1.93 Å, and the conformation of the substrates is staggered, the dihedral angle of the substituents on the two carbons (θ_3, see Figure 8) is 59°. Transition state $\mathbf{TS}_{R1}$ has very similar geometry around the forming C–C bond compared to $\mathbf{TS}_{S1}$: the C–C bond distance is 1.93 Å and θ_3 is 60°. Also the hydrogen bond distances to the catalyst are very similar, within 0.05 Å. The difference lies rather in the orientation of the phenyl ring of benzaldehyde. For $\mathbf{TS}_{S1}$, it points in the direction of the phenyl of the thiourea, whereas in $\mathbf{TS}_{R1}$ the aldehyde substituent points in direction of the methyl ether of the catalyst. None of these interactions represent severe sterics, but these observations might be enough to explain the small energy difference between the two transition states, in agreement with the observed selectivity.

The two torsional angles θ_1 and θ_2 as defined in Figure 8 can function as good indicators of the strain imposed on the catalyst at the transition states. In the free catalyst in the open conformation, these angles are calculated to be 152° and 100°, respectively, in agreement to those found by Burgi and Baiker for cinchonidine (154° and 101°).[18c]

We note that the conformational change of the catalyst is quite small in all the calculated transition states: θ_1 is 5°–15° larger than in the free catalyst indicating that the catalyst has to open up a little more to afford beneficial hydrogen bonding to the quinuclidinium. The deviation for θ_2 is smaller, –1°–7°.

The transition states $\mathbf{TS}_{S2}$ and $\mathbf{TS}_{R2}$ have higher energies compared to $\mathbf{TS}_{S1}$ (+3.7 and +3.9 kcal mol^{-1}, respectively). One reason for this is that they have to adopt a less staggered conformation about the forming C–C bond. θ_3 is 42° and 50° for the two transition states, respectively. The critical C–C bond distance is longer than for $\mathbf{TS}_{S1}$ (2.03 Å *vs.* 1.93 Å) and the hydrogen bond distances to the thiourea are slightly longer, indicating a lower transition state stabilization.

The energies of the *anti* conformation ($\mathbf{TS}_{S3}$ and $\mathbf{TS}_{R3}$) are significantly higher than for the other transition states (+6.8 and +7.3 kcal mol^{-1}, respectively, compared to $\mathbf{TS}_{S1}$). This is mainly due to the arrange-

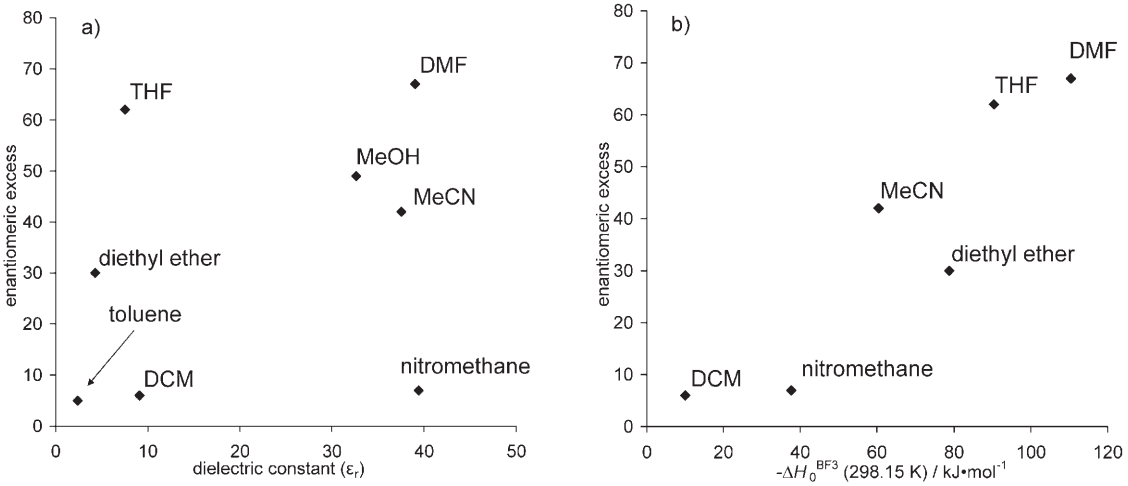

Figure 7. Enantiomeric excess of nitroalcohol **3** *vs.* dielectric constant and Lewis basicity of the solvent.

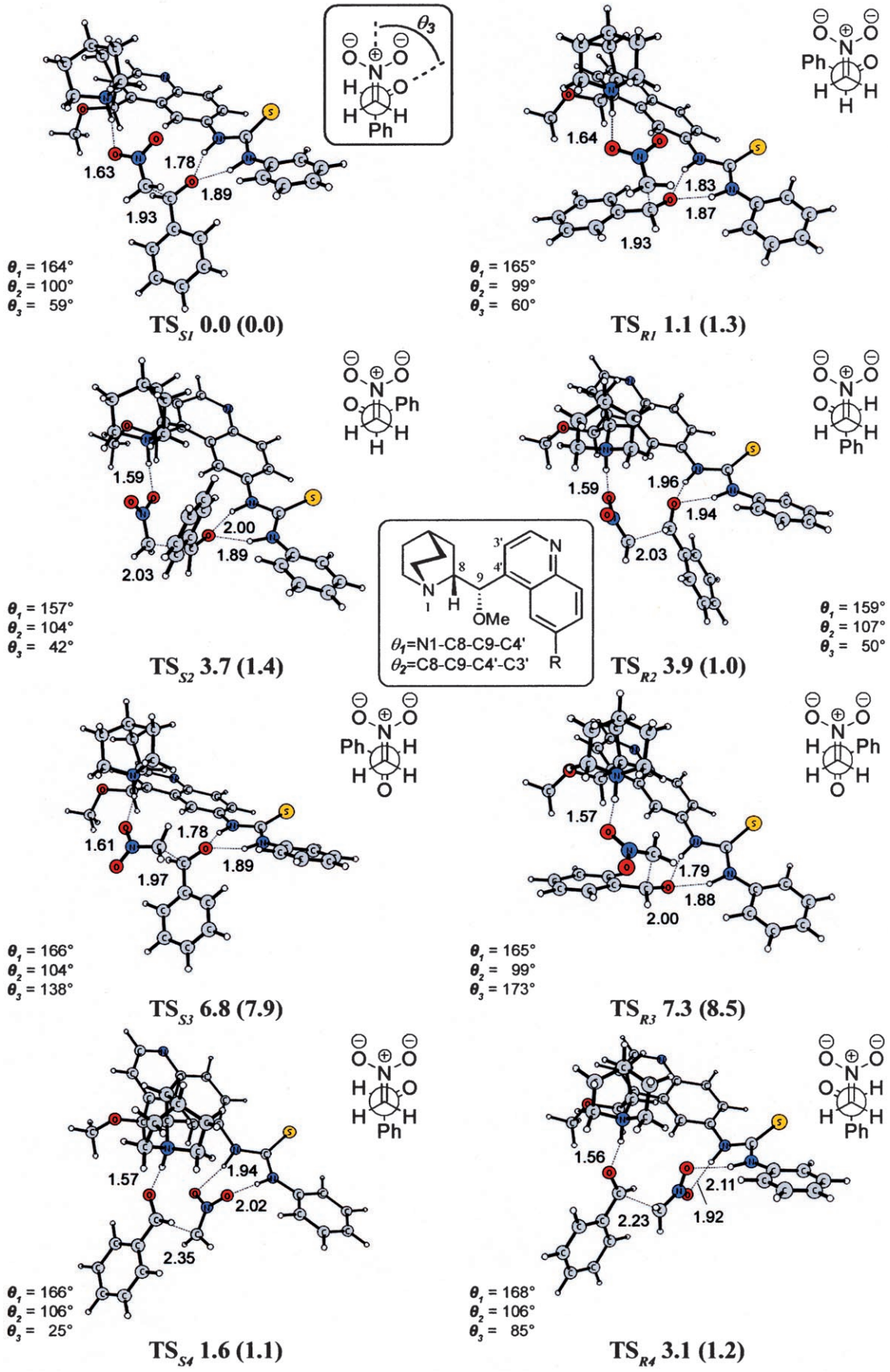

ment of the substrates being far from the optimal staggered conformation. Moreover, the enforced geometry of the hydrogen bonding between the negatively charged nitro group and the quinuclidinium is poor.

For the transition states of Pathway B ($\mathbf{TS}_{S4}$ and $\mathbf{TS}_{R4}$), the nitro group forms two hydrogen bonds to the thiourea moiety, while the developing negative charge at the aldehyde is interacting with the positive charge of the quinuclidinium. This arrangement results in an almost eclipsed conformation about the forming C–C bond, which yields higher transition state energies (+1.6 and +3.1 kcal mol^{-1}, respectively, compared to $\mathbf{TS}_{S1}$).

For the six lowest-lying transition states ($\mathbf{TS}_{S1}$, $\mathbf{TS}_{R1}$, $\mathbf{TS}_{S2}$, $\mathbf{TS}_{R2}$, $\mathbf{TS}_{S4}$, and $\mathbf{TS}_{R4}$), we have reoptimized the structures using catalyst **6**, which has additional trifluoromethyl substituents at the thiourea part. The energetic results are reported in Table 1.

As expected, the overall geometries of the transition states are very similar to the ones without the trifluoromethyl substituents. However, a non-negligible effect on the calculated energies can be detected. Most significantly, adding these two CF_3 groups to the catalyst increases somewhat the steric interactions between the two phenyls in $\mathbf{TSf}_{S1}$, whereas $\mathbf{TSf}_{R1}$ is unaffected. As a result of this, the energy difference between these two lowest-lying transition states drops from 1.1 to 0.0 kcal mol^{-1}, i.e., they become degenerate. The geometries of these two transition states are shown in Figure 9.

Table 1. Summary of calculated relative transition state energies (kcal mol^{-1}) for the C–C bond forming step. Values include solvation effects (gas phase values in parentheses).

	Catalyst **5**	Catalyst **6**
Pathway A		
S1	0.0 (0.0)	0.0 (0.0)
S2	3.7 (1.4)	1.8 (1.6)
S3	6.8 (7.9)	-
R1	1.1 (1.3)	0.0 (0.6)
R2	3.9 (1.0)	5.3 (0.8)
R3	7.3 (8.5)	-
Pathway B		
S4	1.6 (1.1)	3.3 (0.8)
R4	3.1 (1.2)	4.6 (1.1)

These results are still consistent with the experimental findings in that the energies of the transition states leading to the opposite enantiomers must be close, such that different solvents can significantly alter the difference.

It should be mentioned here that adding a benzyloxy substituent on C-9 to catalyst **6** (originally present in **1**) did not affect the calculated energetics significantly. The difference between $\mathbf{TS}_{S1}$ and $\mathbf{TS}_{R1}$ becomes now 0.2 kcal mol^{-1} (compared to 0.0 kcal mol^{-1} for catalyst **6**), verifying the initial assumption that the C-9 ether does not play any major role in the stereoselection.

◀ **Figure 8.** Optimized transition states for Pathway A ($\mathbf{TS}_{S1}$–$\mathbf{TS}_{R3}$) and Pathway B ($\mathbf{TS}_{S4}$ and $\mathbf{TS}_{R4}$). Distances in Ångström for the forming C–C bond and the three hydrogen bonds between the catalyst and the substrates. Insets show the corresponding Newman projection along the forming C–C bond. Framed insets define the dihedral angles specified. Relative energies (kcal mol^{-1}) including solvation correction are given in the labels (gas phase values in parentheses).

Conclusions

In the present paper, we have used DFT calculations to study the reaction mechanism and the enantiose-

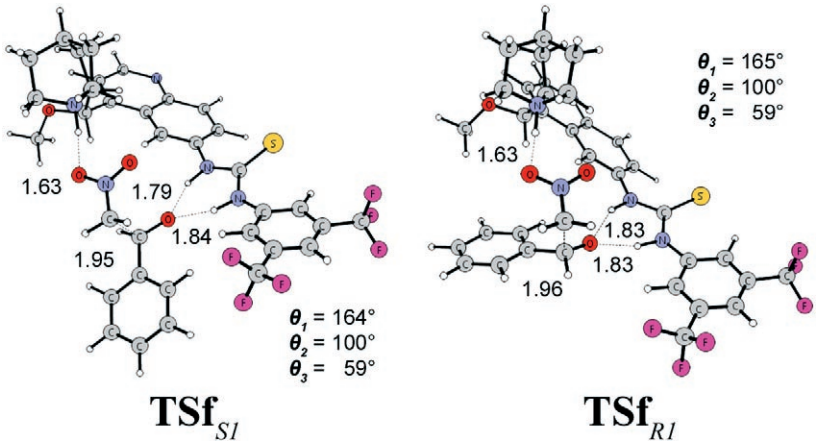

Figure 9. The energetically most accessible transition states using catalyst **6**.

lectivity of the reaction of benzaldehyde (**2**) with nitromethane catalyzed by *Cinchona* thiourea **5**.

Our results support the proposed reaction mechanism in which nitromethane deprotonation and aldehyde complexation are followed by a C–C bond formation step and subsequent protonation of the resulting alkoxide. Two possible routes to C–C bond formation (Pathway A and B in Scheme 3) involving opposite coordination patterns of the hydrogen bond donors (quinuclidinium and thiourea) and acceptors (nitromethide anion and aldehyde) were found. Pathway A is slightly preferred over Pathway B.

Table 1 summarizes the calculated energies for the different transition states of the C–C bond formation step. In both pathways we see a slight preference for the *S* enantiomer, in agreement with the experimental findings. The calculated magnitude of the energy difference between the lowest-lying transition states leading to the opposite enantiomers is very small (or non-existing), which is consistent with the previously discussed solvent effect. Slight differences in the interaction of the solvent with the pro-*R* and pro-*S* transition states can thus affect this small energy difference resulting in changes in the enantioselectivity. It is worth pointing out that the CPCM model we employed in this computational study can only account for dielectric effects of the solvent in an averaged way. Therefore, the experimentally determined solvent dependence of the enantioselectivity cannot be satisfactorily explained with such an implicit model.

Experimental Section

General Remarks

NMR spectra (^{1}H and ^{13}C) were measured using a Bruker ARX 400 MHz spectrometer. High-resolution mass spectra were recorded on a JEOL JMS-SX/SX 102A tandem mass spectrometer. Infrared spectra were performed on a Bruker IFS 28 FT spectrometer. Thiourea **7** was prepared according to Deng et al.[19]

Methyl Quinidine (MeQD)

To a solution of quinidine (2 g, 6.2 mmol) in DMF (20 mL), sodium hydride (60% suspension in mineral oil, 618 mg, 15.5 mmol) was added portionwise. The resulting mixture was stirred for 1 h then methyl iodide (423 μL, 6.8 mmol) was added dropwise. Stirring was continued overnight, the reaction was quenched with brine (10 mL) and the mixture was extracted with EtOAc (2×20 mL). The combined organic layers were washed with brine (3×5 mL), dried on $MgSO_4$ and concentrated under vacuum. Purification by column chromatography (EtOAc/MeOH, 9:1) afforded the title compound (yield: 1.75 g, 84%) as a pale yellow oil with spectral data matching those reported in the literature.[25] ^{1}H NMR ($CDCl_3$): $\delta = 8.74$ (d, $J = 4.5$ Hz, 1H), 8.02 (d, $J = 9.2$ Hz, 1H), 7.42 (d, $J = 4.5$ Hz, 1H), 7.37 (dd, $J = 9.2$, 2.6 Hz, 1H), 7.27 (m, 1H), 6.09 (m, 1H), 5.10–5.05 (m, 3H), 3.92 (s, 3H), 3.32 (s, 3H), 3.30 (m, 1H), 3.00–2.77 (m, 4H), 2.24 (m, 1H), 2.03 (m, 1H), 1.72 (bs, 1H), 1.47 (m, 2H), 1.21 (m, 1H).

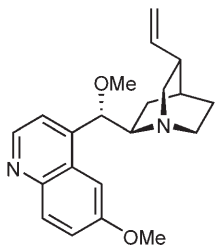

Methyl Cupreidine (MeCPD)

To a solution of **MeQD** (1.74 g, 5.2 mmol) in DMF (30 mL), sodium ethanethiolate (1.73 g, 20.6 mmol) was added. The

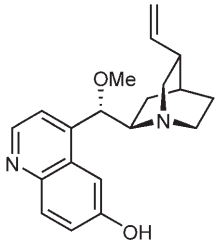

mixture was warmed to 110 °C and stirring was continued for 20 h. After cooling, the reaction was quenched with satd. NH_4Cl (35 mL) and water (30 mL). The resulting mixture was extracted with EtOAc (2×150 mL) and the combined organic layers were washed with brine (3×30 mL), dried on MgSO4 and concentrated under vacuum. Purification by flash chromatography (EtOAc/MeOH, 9:1+1% Et_3N) afforded the title compound as a yellow foam; yield: 1.08 g (64%). ^{1}H NMR ($CDCl_3$): $\delta = 8.70$ (d, $J = 4.5$ Hz, 1H0, 8.03 (d, $J = 9.1$ Hz, 1H), 7.94 (bs, 1H), 7.82 (d, $J = 2.5$ Hz, 1H), 7.39 (d, $J = 4.5$ Hz, 1H), 7.37 (dd, $J = 9.1$, 2.5 Hz, 1H), 6.12 (m, 1H), 5.30 (bs, 1H), 5.16–5.11 (m, 2H), 3.60 (m, 1H), 3.21 (s, 3H), 3.12–2.87 (m, 4H), 2.35 (m, 1H), 2.25 (m, 1H), 1.80 (bs, 1H), 1.62 (m, 1H), 1.47 (m, 1H), 1.12 (m, 1H); ^{13}C NMR ($CDCl_3$): $\delta = 156.73$, 146.49, 143.54, 143.04, 139.83, 131.27, 127.73, 123.16, 117.88, 115.02, 106.43, 81.04, 58.76, 56.84, 49.54, 49.11, 39.58, 28.02, 25.68, 19.82; IR (NaCl): $\nu_{max} = 3072$, 2938, 2876, 1618, 1509, 1468, 1242, 1120, 1067, 912, 831 cm^{-1}; HR-MS (FAB):$m/z = 325.1921$ ($M+H^+$), calcd. for $[C_{20}H_{25}N_2O_2]^+$: 325.1911.

Aryl Triflate (8)

To a solution of **MeCPD** (1.10 g, 3.42 mmol) in CH_2Cl_2 (25 mL), *N*-phenyl-bis(trifluoromethanesulfonimide) (1.22 g, 3.42 mmol) and 4-dimethylaminopyridine (50 mg, 0.41 mmol) were added and the resulting mixture was stirred overnight. The solvent was then evaporated and the residue was diluted with EtOAc (100 mL), extracted with saturated Na_2CO_3 (3×50 mL), dried on $MgSO_4$ and concentrated under vacuum. Purification by flash chromatography (0–5% MeOH in EtOAc) afforded the title compound as a pale

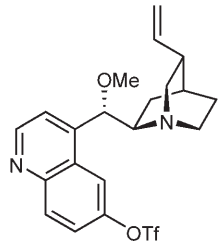

yellow oil; yield: 1.01 g (65%). ^{1}H NMR ($CDCl_3$): $\delta = 8.96$ (d, $J = 4.5$ Hz, 1H), 8.23 (d, $J = 9.3$ Hz, 1H), 8.18 (d, $J = 2.6$ Hz, 1H), 7.60 (dd, $J = 9.3$, 2.6 Hz, 1H), 7.52 (d, $J = 4.5$ Hz, 1H), 6.05 (m, 1H), 5.12–5.07 (m, 2H), 4.91 (d, $J = 5.7$ Hz, 1H), 3.31 (s, 3H), 3.12–3.06 (m, 2H), 2.95 (m, 1H), 2.75 (m, 2H), 2.27 (m, 1H), 1.97 (m, 1H), 1.78 (bs, 1H), 1.53 (m, 2H), 1.39 (m, 1H); ^{13}C NMR ($CDCl_3$): $\delta = 151.07$, 147.29, 146.85, 146.64, 140.15, 132.96, 126.53, 122.52, 120.41, 118.73 (*q*, $J = 321$ Hz), 115.96, 114.54, 83.71, 60.43, 57.30, 49.66, 48.99, 39.61, 27.78, 26.11, 22.77; IR (NaCl): $\nu_{max} =$ 2937, 1508, 1423, 1213, 1140, 928, 846, 829 cm^{-1}; HR-MS (FAB): $m/z = 325.1921$ ($M+H^+$), calcd. for $[C_{21}H_{24}F_3N_2O_4S]^+$: 457.1403.

Aminoquinoline (9)

To a warm (66 °C) solution of triflate **8** (0.96 g, 2.09 mmol) in THF (20 mL) were added $Pd(OAc)_2$ (27 mg, 0.12 mmol), (±)-BINAP (118 mg, 0.19 mmol), Cs_2CO_3 (955 mg,

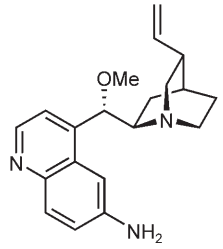

2.93 mmol) and benzophenone imine (421 μL, 2.51 mmol). The mixture was stirred for 24 h then was allowed to cool to room temperature, filtered over a short pad of Celite and eluted with CH_2Cl_2. The filtrate was concentrated under vacuum and the residue was redissolved in THF (10 mL) and 10% acqueous citric acid (20 mL). The mixture was stirred at room temperature for 24 h then EtOAc (100 mL) and satd. Na_2CO_3 (100 mL) were added. The layers were separated and the water layer was washed with EtOAc (50 mL). The combined organic layers were extracted with 1 N HCl (2×75 mL). The combined acidic water layers were washed with CH_2Cl_2 (3×50 mL). Ethyl acetate (100 mL) was added and the mixture was made alkaline by the addition of saturated Na_2CO_3 (~150 mL) and extracted. The water layer was then further extracted with EtOAc (3× 100 mL). The combined organic layers were washed with brine (2×50 mL), dried on $MgSO_4$ and concentrated under vacuum. Purification by flash chromatography (EtOAc/MeOH, 9:1+1% ammonium hydroxide) afforded the title compound as a white foam; yield: 230 mg (34%). ^{1}H NMR ($CDCl_3$): $\delta = 8.58$ (d, $J = 4.5$ Hz, 1H), 7.88 (d, $J = 9.6$ Hz, 1H), 7.30 (d, $J = 4.5$ Hz, 1H), 7.06 (m, 2H), 6.11–6.02 (m, 1H), 5.05–4.96 (m, 3H), 4.19 (bs, 2H), 3.28 (m, 1H), 3.25 (s, 3H), 2.92–2.86 (m, 3H), 2.72 (m, 1H), 2.19 (m, 1H), 2.06 (m, 1H), 1.68 (bs, 1H), 1.46–1.39 (m, 2H), 1.08 (m, 1H); ^{13}C NMR ($CDCl_3$): $\delta = 146.01$, 144.91, 143.23, 142.92, 140.78, 131.27, 127.68, 120.83, 118.27, 114.20, 102.60, 83.01, 59.15, 56.94, 49.87, 49.40, 40.13, 28.14, 26.36, 20.75; IR (NaCl): $\nu_{max} = 3335$, 3208, 2937, 2874, 1622, 1513, 1119, 1067, 910, 828 cm^{-1}; HR-MS (FAB): $m/z = 324.2086$ ($M+H^+$), calcd. for $[C_{20}H_{26}N_3O]^+$: 324.2070.

Thiourea (5)

To a solution of amine **9** (64 mg, 0.2 mmol) in THF (5 mL) was added phenyl isothiocyanate (24 μL, 0.2 mmol) and the

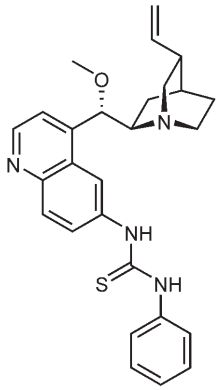

mixture was stirred for 24 h at room temperature. The THF was removed under reduced pressure and the crude product was purified by flash chromatography (EtOAc/MeOH, 95:5+0.5% Et_3N), affording a pale yellow foam; yield: 40 mg (45%). ^{1}H NMR ($CDCl_3$): $\delta = 8.85$ (d, $J = 4.5$ Hz, 1H), 8.22 (d, $J = 1.6$ Hz, 1H), 8.09 (d, $J = 9.1$ Hz, 1H), 7.91 (dd, $J = 9.1$, 2.1 Hz, 1H), 7.45 (d, $J = 4.5$ Hz, 1H), 7.39 (m, 3H), 7.26 (m, 1H), 6.10–6.01 (m, 1H), 5.09 (m, 3H), 3.23 (s, 3H + m, 1H), 3.07 (m, 1H), 2.91–2.85 (m, 2H), 2.65 (m, 1H), 2.22 (m, 1H), 2.05 (m, 1H), 1.73 (bs, 1H), 1.45 (m, 2H), 1.26 (m, 1H); ^{13}C NMR ($CDCl_3$): $\delta = 79.88$, 149.69, 146.42, 145.59, 140.43, 136.91, 136.11, 130.82, 129.54, 126.91, 126.69, 126.39, 125.14, 118.92, 117.55, 114.47, 82.82, 59.74, 57.12, 50.32, 49.73, 49.30, 39.88, 27.96, 26.09, 21.31; IR ($CHCl_3$): $\nu_{max} = 3332$, 2921, 2360, 1593, 1121 cm^{-1}; $[\alpha]_D^{22}$: +151.4 (*c* 1.00, $CHCl_3$); HR-MS (FAB): $m/z = 459.2217$, ($M+H^+$), calcd. for $[C_{27}H_{31}N_4OS]^+$: 459.2213.

Supporting Information

Complete citation for ref.[16] Kinetic profiles for catalyst **1**. Cartesian coordinates of the reported transition state structures.

Acknowledgements

Jan Geenevasen is gratefully acknowledged for his precious help with the kinetic measurements. Dr. Enrico Burello is ac-

knowledged for stimulating discussions about the solvent effects. T.M. gratefully acknowledges the National Research School Combination Catalysis (NRSC-C) for financial support. F.H. gratefully acknowledges financial support from: The Swedish National Research Council, The Wenner-Gren Foundations, The Carl Trygger Foundation, and The Magn Bergvall Foundation.

References

[1] For general reviews, see: a) G. Rosini, in: *Comprehensive Organic Synthesis Vol. 2*, (Eds. B. M. Trost, I. Flemig, C. H. Heatcock), Pergamon, New York, **1991**, pp 321–340; b) F. A. Luzzio, *Tetrahedron* **2001**, *57*, 915–945.

[2] a) H. Sasai, T. Suzuki, S. Arai, M. Shibasaki, *J. Am. Chem. Soc.* **1992**, *114*, 4418–4420; b) M. Shibasaki, N. Yoshikawa, *Chem. Rev.* **2002**, *102*, 2187–2209.

[3] For recent reviews on the asymmetric Henry reaction, see: a) C. Palomo, M. Oiarbide, A. Laso. *Eur. J. Org. Chem.* **2007**, 2561–2574; b) J. Boruwa, N. Gogoi, P. P. Saikia, N. C. Barua, *Tetrahedron: Asymmetry* **2006**, *24*, 3315–3326; c) C. Palomo, M. Oiarbide, A. Mielgo, *Angew. Chem. Int. Ed.* **2004**, *43*, 5442–5444.

[4] For early studies (with enantiomeric excesses not exceeding 52%), see: a) R. Chinchilla, C. Najera, P. Sanchez-Agullo, *Tetrahedron: Asymmetry* **1994**, *5*, 1393–1402; b) Y. Misumi, R. A. Bulman, K. Matsumoto, *Heterocycles* **2002**, *56*, 599–605; c) M. T. Allingham, A. Howard-Jones, P. J. Murphy, D. A. Thomas, P. W. R. Caulkett, *Tetrahedron Lett.* **2003**, *44*, 8677–8680.

[5] For a short review, see: T. Marcelli, J. H. van Maarseveen, H. Hiemstra, *Angew. Chem. Int. Ed.* **2006**, *45*, 7496–7504.

[6] T. Marcelli, R. N. S. van der Haas, J. H. van Maarseveen, H. Hiemstra, *Synlett* **2005**, 2817–2819.

[7] For reviews, see: a) S. J. Connon, *Chem. Eur. J.* **2006**, *12*, 5418–5427; b) M. S. Taylor, E. N. Jacobsen, *Angew. Chem. Int. Ed.* **2006**, *45*, 1520–1543.

[8] T. Marcelli, R. N. S. van der Haas, J. H. van Maarseveen, H. Hiemstra, *Angew. Chem. Int. Ed.* **2006**, *45*, 929–931.

[9] a) Y. Sohtome, Y. Hashimoto, K. Nagasawa, *Adv. Synth. Cat.* **2005**, *347*, 1643–1648; b) Y. Sohtome, Y. Hashimoto, K. Nagasawa, *Eur. J. Org. Chem.* **2006**, *13*, 2894–2897; c) Y. Sohtome, N. Takemura, K. Takada, R. Takagi, T. Iguchi, K. Nagasawa, *Chem. Asian J.*, **2007**, DOI: 10.1002/asia.200700145.

[10] H. M. Li, B. M. Wang. L. Deng, *J. Am. Chem. Soc.* **2006**, *128*, 732–733.

[11] a) T. Purkarthofer, K. Gruber, M. Gruber-Khadjawi, K. Waich, W. Skranc, D. Mink, H. Griengl, *Angew. Chem. Int. Ed.* **2006**, *45*, 3454–3456; b) M. Gruber-Khadjawi, T. Purkarthofer, W. Skranc, H. Griengl, *Adv. Synth. Cat.* **2007**, *349*, 1445–1450.

[12] For general reviews, see: a) P. I. Dalko, L. Moisan, *Angew. Chem. Int. Ed.* **2004**, *43*, 5138–5175; b) P. I. Dalko, L. Moisan, *Angew. Chem. Int. Ed.* **2001**, *40*, 3726–3748; c) J. Seayad, B. List, *Org. Biomol. Chem.* **2005**, *3*, 719–724; d) special issue of *Acc. Chem. Res.* **2004**, *37*, issue 8; e) A. Berkessel, H. Gröger, *Asymmetric Organocatalysis*, Wiley-VCH, Weinheim, **2005**; f) *Enantioselective Organocatalysis*, (Ed.: P. I. Dalko), Wiley-VCH, Weinheim, **2007**.

[13] Computational analyses of asymmetric heterogenous hydrogenation employing *Cinchona* alkaloids as surface modifiers are, on the other hand, more abundant. For recent examples, see: a) J. Vayner, K. N. Houk, Y. K. Sun, *J. Am. Chem. Soc.* **2004**, 126, 199–203; b) A. Vargas, T. B. Burgi, A. Baiker, *J. Catal.* **2004**, *222*, 439–449.

[14] a) C. Lee, W. Yang, R. G. Parr, *Phys. Rev.* **1988**, *B37*, 785; b) A. D. Becke, *Phys. Rev.* **1988**, *A38*, 3098; c) A. D. Becke, *J. Chem. Phys.* **1992**, *96*, 2155; d) A. D. Becke, *J. Chem. Phys.* **1992**, *97*, 9173; e) A. D. Becke, *J. Chem. Phys.* **1993**, *98*, 5648.

[15] a) M. Arno, R. J. Zaragoza, L. R. Domingo, *Tetrahedron: Asymmetry* **2004**, *15*, 1541–1549; b) A. Córdova, H. Sunden, A. Bogevig, M. Johansson, F. Himo, *Chem. Eur. J.* **2004**, *10*, 3673–3684; c) J. Joseph, D. B. Ramachary, E. D. Jemmis, *Org. Biomol. Chem.* **2006**, *4*, 2685–2689; d) F. R. Clemente, K. N. Houk, *Angew. Chem. Int. Ed.* **2004**, *43*, 5766–5768; e) A. Bassan, W. Zou, E. Reyes, F. Himo, A. Córdova, *Angew. Chem. Int. Ed.* **2005**, *44*, 7028–7032; f) D. A. Yalalov, S. B. Tsogoeva, S. Schmatz, *Adv. Synth. Cat.* **2006**, *348*, 826–832; g) R. Zhu, D. Zhang, J. Wu, C. Liu, *Tetrahedron: Asymmetry* **2006**, *17*, 1611–1616; h) R. Gordillo, K. N. Houk, *J. Am. Chem. Soc.* **2006**, *128*, 3543–3553.

[16] M. J. Frisch et al., *Gaussian '03* (Revision A.1), Gaussian Inc., Pittsburgh, PA, **2004**.

[17] a) M. Cossi, N. Rega, G. Scalmani, V. Barone, *J. Comput. Chem.* **2003**, *24*, 669–681; b) V. Barone, M. Cossi, *J. Phys. Chem. A* **1998**, *102*, 1995–2001.

[18] a) G. D. H. Dijkstra, R. M. Kellogg, H. Wynberg, *Recl. Trav. Chim. Pays-Bas*, **1989**, *108*, 95; b) G. D. H. Dijkstra, R. M. Kellogg, H. Wynberg, J. S. Svendsen, I. Marko, K. B. Sharpless, *J. Am. Chem. Soc.* **1989**, *111*, 8069–8076; c) T. Bürgi, A. Baiker, *J. Am. Chem. Soc.* **1998**, *120*, 12920–12926.

[19] J. Song, Y. Wang, L. Deng, *J. Am. Chem. Soc.* **2006**, *128*, 6048–6049.

[20] H. Li, Y. Wang, L. Tang, F. Wu, X. Liu, C. Guo, B. M. Foxman, L. Deng, *Angew. Chem. Int. Ed.* **2005**, *44*, 105–108.

[21] For a constantly updated table of pK_a values in DMSO, see: http://www.chem.wisc.edu/areas/reich/pKatable/index.htm, and cited references therein.

[22] A. Hamza, G. Schubert, T. Soos, I. Papai, *J. Am. Chem. Soc.* **2006**, *128*, 13151–13160.

[23] P.-C. Maria, J.-F. Gal, *J. Phys. Chem.* **1985**, *89*, 1296–1304.

[24] V. Gutmann, *Coord. Chem. Rev.* **1976**, *18*, 225–255, and references cited therein.

[25] C. D. Papageorgiou, M. A. Cubillo de Dios, S. V. Ley, M. J. Gaunt, *Angew. Chem. Int. Ed.* **2004**, *43*, 4641–4644.

